International Journal of Non-Linear Mechanics 71 (2015) 8–21

Contents lists available at ScienceDirect

International Journal of Non-Linear Mechanics

journal homepage: www.elsevier.com/locate/nlm

Fully non-linear wave models in fiber-reinforced anisotropic incompressible hyperelastic solids

A.F. Cheviakov [a,*], J.-F. Ganghoffer [b], S. St. Jean [a]

[a] Department of Mathematics and Statistics, University of Saskatchewan, Canada
[b] LEMTA, Université de Lorraine, Nancy, France

ARTICLE INFO

Article history:
Received 12 November 2014
Received in revised form
14 January 2015
Accepted 15 January 2015
Available online 29 January 2015

Keywords:
Incompressible hyperelasticity
Fiber-reinforced materials
Symmetries
Exact solutions
Fully non-linear waves

ABSTRACT

Many composite materials, including biological tissues, are modeled as non-linear elastic materials reinforced with elastic fibers. In the current paper, the full set of dynamic equations for finite deformations of incompressible hyperelastic solids containing a single fiber family are considered. Finite-amplitude wave propagation ansätze compatible with the incompressibility condition are employed for a generic fiber family orientation. Corresponding non-linear and linear wave equations are derived. It is shown that for a certain class of constitutive relations, the fiber contribution vanishes when the displacement is independent of the fiber direction.

Point symmetries of the derived wave models are classified with respect to the material parameters and the angle between the fibers and the wave propagation direction. For planar shear waves in materials with a strong fiber contribution, a special wave propagation direction is found for which the non-linear wave equations admit an additional symmetry group. Examples of exact time-dependent solutions are provided in several physical situations, including the evolution of pre-strained configurations and traveling waves.

1. Introduction

The majority of open problems in the theory of elasticity and related areas and applications stem from the essential non-linearity of the governing equations. Starting from the landmark work of Hadamard and Rivlin [19,34], a large number of theoretical results have been obtained in the field of non-linear elastostatics, especially in the case of incompressible materials. The study of non-linear wave propagation in the elastodynamic setting has received significant attention. Substantial work in the theory of non-linear elastic waves in pre-stressed solid bodies relies on the linearization of the equations of non-linear elastodynamics with respect to small perturbations superimposed on a state of homogeneous or inhomogeneous finite strain. The propagation of acoustic waves within finitely deformed elastic materials was first considered in [45], based on the superimposition of small-amplitude oscillations on finite initial homogeneous deformations. This pioneering work was then followed by other contributions, including [3,43,44,46]. It was more specifically shown in those works that pure longitudinal and pure transverse waves can only propagate in the so-called specific directions, depending on material symmetries [7]. A formulation of elastic energy density for an isotropic medium involving small-but-finite amplitude waves, relying on certain approximations, has been developed in [20].

In contrast to the approximate treatment of non-linear models based on the incremental analysis (linear approximation) of the field equations, the more general situation of finite amplitude waves leads to fully non-linear models (e.g., [30]). Fewer theoretical results are available for such models. Fundamental work relevant to this contribution includes that of Carroll [8], where finite-amplitude incompressible elastic waves in non-linear isotropic materials were studied, and linearly polarized motions in one and two dimensions, and circularly polarized transverse waves were considered. The topic of finite amplitude waves in finitely deformed solids is extensively discussed in [38] and references therein. In the last twenty years, much attention has been devoted to classes of materials with specific constitutive relations, such as the neo-Hookean and Mooney–Rivlin hyperelastic materials. Exact solutions of various non-linear elasticity models for specific types of motions have been derived in a number of papers, including [15,36].

The analysis of non-linear wave propagation in pre-strained or pre-stressed elastic solid bodies is of particular interest in a number of mechanical and physical areas including geophysics, electronics, earthquake engineering, composite materials, ultrasonic non-destructive analysis of soft biological tissues. Initial stress and/or strain frequently occurs during the manufacturing and assembly of structural elements, such as composite materials, fiber reinforced solids (including dry textiles). Moreover, non-zero

* Corresponding author.
E-mail address: cheviakov@math.usask.ca (A.F. Cheviakov).

http://dx.doi.org/10.1016/j.ijnonlinmec.2015.01.006
0020-7462/

stress and strain are often naturally present in soft biological tissues such as veins, arteries, muscles, ligaments and tendons (see, e.g., [22]); for instance, skin is in a state of natural tension.

The propagation of non-linear waves in many materials, including soft tissues, may be further complicated by anisotropy effects [42]. The anisotropy of the deformation pattern can be induced, for example, by an initial state of finite deformation, onto which further motions are superimposed, or by the existence of a fibrous microstructure which has preferred directions. Examples of soft biological tissues which display this type of microstructure are arteries (see [1,22,23]) and skin (e.g., [2,35]). The analysis of non-linear waves in soft tissues consisting of a soft matrix reinforced by fibers requires the theory of fiber-reinforced isotropic hyperelastic materials. Various constitutive models of fiber-reinforced materials have been introduced, including models for one and two families of fibers. For such models, the determination of the elastic constants is more involved than in the isotropic case due to the presence of additional anisotropy parameters. Some of these models are reviewed below.

A number of important theoretical results have been obtained for fiber-reinforced material models. A possibility of singular behavior of transversely isotropic (single fiber family) incompressible materials under inhomogeneous shear was discovered in [28]. It was shown that depending on the reinforcement strength, the static stress field may become discontinuous, which is associated with fiber kinking and the loss of ellipticity of the field equations. In [17], equilibrium states of incompressible materials with two parallel families of fibers under shear deformations were considered; it was shown that strain singularities can develop when mechanical differences between the two fibers families are sufficiently large. Practical implications of such singular behaviors in biological and other models have been discussed.

On the side of applications, the topic of non-linear wave propagation in anisotropic media has received considerable attention due to its implication in imaging techniques aiming at accessing mechanical properties or internal visualization of organs (e.g., [48]). A number of imaging techniques have been developed to characterize tissue stiffness *in vivo* by measuring the shear wave speed propagation [37,40,41].

Invariance properties of the governing equations are an important aspect of the theoretical understanding of linear and non-linear physical models. The Lie point symmetry framework and related methods provide systematic ways of study of invariance properties of differential equations (DE) with respect to continuous and discrete symmetry groups. Local symmetries have been widely used to obtain exact solutions of DEs, as symmetry-invariant solutions, or through mappings of known solutions into new ones. Many techniques for exact solution of ordinary and partial differential equations (ODE, PDE), including superposition principles, integral transforms, existence of separated solutions, reduction of order for ODEs, construction of Green's functions, existence of traveling wave solutions, etc., are directly related to symmetry properties of the equations under study. In particular, the invariance under space and time translations validates the traveling wave solution ansatz, which is essential for soliton equations, such as the Korteweg–de Vries equation, the non-linear Schrödinger equation, and the Sine–Gordon equation. Most of the wave equations of physical interest in fact admit larger symmetry groups. For variational PDE systems, local conservation laws and variational symmetries are equivalent through Noether's theorem. This is generally not so for non-variational PDE systems (see, e.g., [4,5,6,31]). An extensive study of the relationship between symmetries and conservation laws appears in [31] and references therein. We note that a number of important equations of mathematical physics, including the Khokhlov–Zabolotskaya and the integrable Kadomtsev–Petviashvili and models, arise in non-linear elasticity context (e.g., [13]).

Symmetries of the two-dimensional Ciarlet–Mooney–Rivlin model of compressible isotropic hyperelastic materials have been analyzed in [9]. A special value of the traveling wave speed has been found for which the non-linear Ciarlet–Mooney–Rivlin equations admit an additional infinite set of point symmetries. A family of essentially two-dimensional traveling wave solutions has been derived for that case. An overview of related recent results based on the application of symmetry methods to elastodynamics equations can also be found in [9].

The current contribution is concerned with the theoretical study of fully non-linear wave propagation models in fiber-reinforced hyperelastic incompressible materials, with a specific goal of finding closed-form time-dependent exact solutions in two spatial dimensions. In the present work, we restrict our attention to the case of a single family of fibers. Wave propagation ansätze compatible with the incompressibility condition, for a general fiber family orientation, are used. The work is based on the Lie point symmetry classification of the governing equations. It is planned to address the more general situation of two families of fibers, which is necessary, for example, for an adequate description of biological tissues [22], in subsequent work.

An outline of the present contribution is as follows. The equations of motion for incompressible hyperelastic solids reinforced with a single family of fibers are reviewed in Section 2. Several constitutive relations are discussed. In our work, we restrict our attention to incompressible Mooney–Rivlin-type materials.

In Section 3, motions with a special orientation with respect to the fiber family are considered. In particular, in the general fully non-linear setting, a theorem is proven stating that if the displacement is independent of the fiber direction, then the fiber-dependent invariant I_4 is a constant. It follows that in models where a constitutive relation for the fiber-reinforced material involves a fiber contribution only through I_4, motions with the indicated displacements will not "feel" the presence of fibers. Examples of such motions are considered in the following sections. A similar statement in a totally different context of the incremental analysis and linearized equations has been made in [29]. There, it is noted that "…the shear wave solution involving only deformation in the plane of isotropy is not affected by anisotropic term in the constitutive equation". In the current paper, we show that even in the full non-linear setting, motions with displacements independent of the fiber direction are indeed not affected by the anisotropic terms if the constitutive relation only involves the invariant I_4. The effect of anisotropy will still be present if the model involves other fiber-dependent invariants, for example, I_5 (see Section 2).

Fully non-linear anti-plane shear motions, with displacements orthogonal to a plane, are considered in Section 4, for an arbitrary fiber family orientation. Displacements dependent on one and two spatial variables are analyzed. Lie point symmetries are computed in one- and two-dimensional cases. For the two-dimensional case, the displacement satisfies a non-linear wave equation with a differential constraint (cf. [21,25,47]). The loss of hyperbolicity in the model is discussed; a sufficient condition of hyperbolicity is derived. A single non-linear wave equation is derived for one-dimensional transverse wave (s-wave) propagation; its sample numerical solutions are obtained. It is proven that the one-dimensional model admits an extra symmetry for a special fiber orientation. The condition for the existence of the extra symmetry corresponds to the boundary of the domain of model parameters in which the loss of hyperbolicity of the PDE may occur. The additional symmetry is used to construct an exact symmetry-invariant solution describing the degeneration of the parabolic shear into a simple linear shear as $t \to \infty$.

Another situation where displacements are orthogonal to an axis is studied in Section 5, for the general and specific fiber family orientations. Here displacements in the two transverse directions and the hydrostatic pressure satisfy a $1+1$-dimensional non-linear

PDE system. Point symmetries of that system are classified; an additional symmetry is again found for the special fiber orientation. Examples of exact closed-form solutions are obtained for this fully non-linear model in the traveling wave ansatz. (The existence of the latter follows from the symmetry classification.) The first solution example is a bounded deformation traveling in the fiber direction through a pre-stressed medium. The second example is the traveling shear wave where displacements of Lagrangian points follow circles in the plane transverse to the direction of wave propagation.

Importantly, the ansätze considered in the current paper are not limited to linear or plane waves.

The paper is concluded with a discussion in Section 6.

The symmetry computations were performed using `GeM` software package for `Maple` [10].

2. Equations of motion and constitutive relations

In order to set the stage, we recall the main ingredients of hyperelastic models.

Within the paper, boldface notation will be used to denote vector and tensor quantities. Partial derivatives are often denoted by subscripts: $\partial u/\partial x \equiv u_x$.

2.1. Setup and notation

Consider a solid body that at time $t=0$ occupies the spatial region $\overline{\Omega}_0 \subset \mathbb{R}^3$ (reference, or Lagrange configuration). Here Ω_0 is an open bounded connected set having a Lipschitz boundary [11].

The actual position $\mathbf{x}$ of a material point labeled by $\mathbf{X} \in \overline{\Omega}_0$ at time t is given by

$$\mathbf{x} = \boldsymbol{\phi}(\mathbf{X}, t), \quad x^i = \phi^i(\mathbf{X}, t).$$

Coordinates $\mathbf{X}$ in the reference configuration are commonly referred to as Lagrangian coordinates, and actual coordinates $\mathbf{x}$ as Eulerian coordinates. The deformed body occupies an Eulerian domain $\overline{\Omega} = \boldsymbol{\phi}(\overline{\Omega}_0) \subset \mathbb{R}^3$. The velocity of a material point $\mathbf{X}$ is given by

$$\mathbf{v}(\mathbf{X}, t) = \frac{d\mathbf{x}}{dt} \equiv \frac{d\boldsymbol{\phi}}{dt}.$$

The mapping $\boldsymbol{\phi}$ must be sufficiently smooth (the regularity conditions depending on the particular problem). The Jacobian matrix of the coordinate transformation is given by the deformation gradient tensor

$$\mathbf{F}(\mathbf{X}, t) = \nabla \boldsymbol{\phi}, \tag{2.1}$$

with components

$$F^i_j = \frac{\partial \phi^i}{\partial X^j} = F_{ij}. \tag{2.2}$$

Throughout the paper, we use Cartesian coordinates and the flat space metric tensor. The transformation satisfies the orientation preserving condition

$$J = \det \mathbf{F} > 0.$$

We restrict to incompressible materials with $J=1$.

An essential ingredient of the dynamical equations is *the first Piola–Kirchhoff tensor*, given in terms of the Cauchy stress tensor by

$$\mathbf{P} = J\boldsymbol{\sigma}\mathbf{F}^{-T}. \tag{2.3}$$

In (2.3), $(F^{-T})_{ij} \equiv (F^{-1})_{ji}$ is the transpose of the inverse of the deformation gradient.

For *hyperelastic* materials, a scalar valued volumetric strain energy function $W = W(\mathbf{X}, \mathbf{F})$ in the reference configuration is defined, encapsulating all information regarding the material behavior. In the incompressible case, the stress tensor is

$$\mathbf{P} = -p\,\mathbf{F}^{-T} + \rho_0 \frac{\partial W}{\partial \mathbf{F}}, \tag{2.4}$$

or, in components,

$$P^{ij} = -p(F^{-1})^{ji} + \rho_0 \frac{\partial W}{\partial F_{ij}}, \tag{2.5}$$

where $p = p(\mathbf{X}, t)$ is the hydrostatic pressure [26], and $\rho_0 = \rho_0(\mathbf{X})$ is the time-independent body density in the reference configuration. The actual density in Eulerian coordinates $\rho = \rho(\mathbf{X}, t)$ is time-dependent and is given by

$$\rho = \rho_0 / J.$$

For the incompressible case considered in the current work,

$$\rho = \rho_0.$$

2.2. Constitutive relations

Consider the left Cauchy–Green strain tensor $\mathbf{B}$ and the right Cauchy–Green strain tensor $\mathbf{C}$ defined by

$$\mathbf{B} = \mathbf{F}\mathbf{F}^T, \quad B^{ij} = F^i_k F^j_k, \quad \mathbf{C} = \mathbf{F}^T\mathbf{F}, \quad C_{ij} = F^k_i F^k_j. \tag{2.6}$$

Tensors $\mathbf{B}$ and $\mathbf{C}$ have the same sets of eigenvalues, given by the squares of principal stretches: $\lambda_1^2, \lambda_2^2, \lambda_3^2$. The three principal invariants of the Cauchy–Green tensors $\mathbf{B}$ and $\mathbf{C}$ are given by

$$I_1 = \mathrm{Tr}\,\mathbf{B} = F^i_k F^i_k, \quad I_2 = \tfrac{1}{2}[(\mathrm{Tr}\mathbf{B})^2 - \mathrm{Tr}(\mathbf{B}^2)] = \tfrac{1}{2}(I_1^2 - B^{ik}B^{ki}), \quad I_3 = \det \mathbf{B} = J^2. \tag{2.7}$$

For an isotropic homogeneous hyperelastic material, the strain energy density function $W = W(\mathbf{X}, \mathbf{F})$ is given in terms of the invariants I_1, I_2, I_3:

$$W_{iso} = W_{iso}(I_1, I_2, I_3). \tag{2.8}$$

In the current paper, we restrict our attention to Mooney–Rivlin materials, a subclass of Hadamard materials [18,26], for which the constitutive relation is commonly written as

$$W_{iso} = a(I_1 - 3) + b(I_2 - 3), \quad a, b > 0, \tag{2.9}$$

where the constant "-3" can be omitted without loss of generality. The model (2.9) with $b=0$ is referred to as the Neo-Hookean model.

One may consider anisotropic materials involving one or more sets of fibers. Consider a single fiber bundle, a collection of fibers oriented along a unit vector $\mathbf{A} = \mathbf{A}(\mathbf{X})$ in the reference configuration Ω_0. In the actual configuration, the fiber direction at $\mathbf{x}, t$ is given by unit vectors

$$\mathbf{a} = \mathbf{a}(\mathbf{X}, t) = \mathbf{F}\mathbf{A}/|\mathbf{F}\mathbf{A}| = \mathbf{F}\mathbf{A}/\lambda, \tag{2.10}$$

where $\lambda = |\mathbf{F}\mathbf{A}|$ is the fiber stretch.

The reinforcement of an isotropic hyperelastic material by a fiber bundle is modeled by adding an anisotropic term to the strain energy density corresponding to the fiber bundle [1,12,22]; that is, the strain energy density takes the form

$$W = W_{iso} + W_{aniso}, \tag{2.11}$$

where W_{iso} corresponds to the isotropic matrix, and W_{aniso} captures the anisotropic effects of the fiber bundle.

The anisotropic strain energy is, in general, constructed from additional invariants corresponding to the fiber behavior,

$$I_4 = \mathbf{A}^T\mathbf{C}\mathbf{A}, \tag{2.12a}$$

$$I_5 = \mathbf{A}^T\mathbf{C}^2\mathbf{A}. \tag{2.12b}$$

Here, I_4 accounts for deformations that modify the length of the fiber, with $I_4 > 1$ corresponding to fibers in extension, and $I_4 < 1$ to

fibers in compression. The invariant I_5 is related to the effect of the fiber on the shear response in the material [12,27]. The anisotropic component of the strain energy density is consequently modeled as a function of the invariants I_4 and I_5,

$$W_{aniso} = f(I_4 - 1,\ I_5 - 1), \quad f(0,0) = 0, \tag{2.13}$$

where the "-1" are normalization constants. One of the simplest models of the anisotropic strain energy density is given by the "standard reinforcing model"

$$W_{aniso} = c(I_4 - 1)^2, \tag{2.14}$$

where $c = \text{const} > 0$ is a material parameter [14,24,42].

The Gasser–Holzapfel–Ogden model is a model of an artery that is proposed by Holzapfel, Gasser, and Ogden [22] (see also [23]), in which the isotropic strain energy density is Neo-Hookean, and the anisotropic strain energy density for a single fiber family is of the form

$$W_{aniso} = \frac{k^1}{k^2}\left(e^{k^2(I_4-1)^2} - 1\right), \tag{2.15}$$

where k^1 and k^2 are material parameters.

An additional incompressible artery model has been suggested in [1], where the isotropic component is also Neo-Hookean, and the anisotropic component has a non-linear polynomial form

$$W_{aniso} = \sum_{k=2}^{n} c^k (I_4 - 1)^k. \tag{2.16}$$

In (2.16), c^k are material constants to be determined, and n is chosen appropriately for accurate data fitting. The polynomial form (2.16) has been used with $n=6$ in [1] to optimize finite element computations.

Horgan and Saccomandi [24] derive two anisotropic strain energy densities to account for the limited extensibility of fibers as

$$W_{aniso} = -\mu k^1 \left((I_4 - 1) + k^1 \ln\left(1 - \frac{I_4 - 1}{k^1}\right)\right), \tag{2.17}$$

$$W_{aniso} = -\mu k^2 \ln\left(1 - \frac{(I_4 - 1)^2}{k^2}\right), \tag{2.18}$$

where μ is a shear modulus measuring the degree of anisotropy, and k^1 and k^2 are constants that measure rigidity of the fiber reinforcement. Note that $I_4 - 1 < k^i$, $i=1,2$, such that the stress $\mathbf{P}$ is finite.

A number of models of shear response in fiber-reinforced materials involving the invariant I_5 have been studied in, e.g., [27,29]. Namani and Bayly [29] study shear waves in anisotropic tissue, in which the isotropic strain energy density is that of a compressible Neo-Hookean material, while the anisotropic strain energy density is

$$W_{aniso} = c(I_5 - (I_4)^2), \tag{2.19}$$

where c is a material parameter.

An anisotropic viscoelastic model involving neo-Hookean isotropic and the standard reinforcing model anisotropic energy density components, (2.9) ($b=0$) and (2.14), with an additional anisotropic viscous constitutive term, was considered in [16].

A practically important generalization of the above framework lies in the consideration of two families of parallel fibers. In this case, one generally considers anisotropic strain energy density functions depending on five fiber invariants $I_4, \ldots, I_8$ [42]. A common anisotropic constitutive model is given by the standard quadratic reinforcing model using only a single fiber invariant for each family (see, e.g., [17]), of which (2.14) is a special case.

2.3. Equations of motion

The full system of equations of motion of an incompressible hyperelastic material in three dimensions is given by

$$J = \det \mathbf{F} = 1, \tag{2.20a}$$

$$\rho_0 \mathbf{x}_{tt} = \text{div}_{(X)} \mathbf{P} + \rho_0 \mathbf{R}, \tag{2.20b}$$

$$\mathbf{P} = -p\ \mathbf{F}^{-T} + \rho_0 \frac{\partial W}{\partial \mathbf{F}}, \tag{2.20c}$$

Eq. (2.20b) expresses the balance of momentum for an infinitesimal volume in the reference configuration; $\mathbf{R} = \mathbf{R}(\mathbf{X}, t)$ is the total body force per unit mass; divergence is taken with respect to material coordinates and is given by

$$(\text{div}_{(X)} \mathbf{P})^i = \frac{\partial P^{ij}}{\partial X^j}.$$

Another necessary equation $\mathbf{F}\mathbf{P}^T = \mathbf{P}\mathbf{F}^T$ is equivalent to the Cauchy stress tensor symmetry condition $\boldsymbol{\sigma} = \boldsymbol{\sigma}^T$ and expresses the balance of angular momentum in terms of the nominal stress. For isotropic elastic materials, it can be shown (see, e.g., [9]) that this symmetry condition is identically satisfied.

The anisotropic constitutive model used in this work is as follows. We start from a general model

$$W = W_{iso}(I_1, I_2) + W_{aniso}(I_4, I_5). \tag{2.21}$$

Then we consider in greater detail a model involving Mooney–Rivlin isotropic strain energy density (2.9), and the quadratic anisotropic strain energy density (2.14), that is,

$$W = aI_1 + bI_2 + q(I_4 - 1)^2, \tag{2.22}$$

where $a,\ b,\ q > 0$ are constant material parameters. The first two terms in (2.22) correspond to the classical isotropic behavior given by Mooney–Rivlin model, which is adequate, for example, for rubbers. The last term represents the standard quadratic reinforcing model [27].

Remark 1. It is important to note that in the case of zero forcing or when external forces are conservative, equations of motion (2.20a), (2.20b) follow from a variational principle [32].

3. Motions with a special orientation with respect to the fiber family

Consider the anisotropic part of the strain energy density given by (2.21). Denote the push-forward of the material vector $\mathbf{A}$ by the transformation gradient and the right Cauchy–Green tensor by vectors

$$\mathbf{q} = \mathbf{F}\mathbf{A}, \quad \mathbf{w} = \mathbf{C}\mathbf{A}. \tag{3.1}$$

In particular, $\mathbf{q}$ is directed along the fibers in the actual configuration. Due to the symmetry of $\mathbf{C}$, it is easy to see that the invariants (2.12) are given by

$$I_4 = \mathbf{q}^T\mathbf{q} = |\mathbf{q}|^2; \quad I_5 = \mathbf{w}^T\mathbf{w} = |\mathbf{w}|^2. \tag{3.2}$$

The following examples are of importance for the future analysis.

3.1. Displacement orthogonal to the fiber direction

As a first example, consider now motions

$$\mathbf{x} = \mathbf{X} + \mathbf{G}, \tag{3.3}$$

such that the displacements $\mathbf{G}=\mathbf{G}(\mathbf{X},t)$ are orthogonal to the fibers:

$$\mathbf{G}^T\mathbf{A}=0.$$

Suppose that fibers are in the direction of X^1,

$$\mathbf{A}=[1\ \ 0\ \ 0]^T. \tag{3.4}$$

Then one has, for the motions indicated above,

$$\mathbf{G}=\begin{bmatrix}0\\ G^2(X^1,X^2,X^3,t)\\ G^3(X^1,X^2,X^3,t)\end{bmatrix}. \tag{3.5}$$

The vector $\mathbf{q}$ in (3.1) becomes

$$\mathbf{q}=\mathbf{F}\mathbf{A}=\left[1,\frac{\partial G^2}{\partial X^1},\frac{\partial G^3}{\partial X^1}\right]^T,$$

and hence

$$I_4=1+\left(\frac{\partial G^2}{\partial X^1}\right)^2+\left(\frac{\partial G^3}{\partial X^1}\right)^2.$$

A similar but more involved expression follows for the invariant I_5.

3.2. Displacement independent of the fiber direction

For the second type of motions of interest, the following simple yet important theorem holds.

Theorem 1. *Consider the motion of the material such that the displacement from the stress-free equilibrium is independent of the fiber direction, i.e., it has the form (3.3) with the displacements independent of the fiber direction* $\boldsymbol{A}$*, in the sense that for all* $\mathbf{X}\in\Omega_0$,

$$(\nabla\mathbf{G})\mathbf{A}=0. \tag{3.6}$$

Then the invariant I_4 *is constant.*

Proof. One has

$$\nabla\mathbf{G}\equiv\mathbf{F}-\mathbf{I},$$

and hence from (3.6),

$$\mathbf{q}=\mathbf{F}\mathbf{A}=\mathbf{A}.$$

In particular, such motions preserve the fiber direction and do not stretch fibers, since $\mathbf{a}=\mathbf{A}$ (cf. (2.10)). For such motions, the first anisotropic invariant I_4 given by (2.12a) and (3.2), reduces to

$$I_4=|\mathbf{A}|^2=1. \qquad \square$$

Remark 2. It is important to note that under the conditions of Theorem 1, the displacement component in the fiber direction does not have to vanish.

Example. Without loss of generality, let the fibers be directed in X^1-direction,

$$\mathbf{A}=[1\ \ 0\ \ 0]^T, \tag{3.7}$$

and consider (in the compressible or incompressible case) fully non-linear motions of the form

$$\mathbf{x}=\begin{bmatrix}X^1+G^1(X^2,X^3,t)\\ X^2+G^2(X^2,X^3,t)\\ X^3+G^3(X^2,X^3,t)\end{bmatrix}. \tag{3.8}$$

The displacement in the fiber direction is non-zero; it is given by $G^1(X^2,X^3,t)$. However the displacements do not depend on X^1, the fiber direction. Then by a direct computation,

$$I_4=\mathbf{q}^T\mathbf{q}\equiv\mathbf{C}_{11}=1,$$

i.e., the fibers do not stretch. However, the invariant dependent on the shear is still of importance: one has $\mathbf{w}=\nabla x^1$, and

$$I_5\equiv(\mathbf{C}^2)_{11}=(\nabla x^1)^T\nabla x^1=1+\left(\frac{\partial G^1}{\partial X^2}\right)^2+\left(\frac{\partial G^1}{\partial X^3}\right)^2.$$

Corollary 1. *For compressible materials, where one has [22]*

$$\overline{\mathbf{F}}=J^{-1/3}\mathbf{F},\quad \overline{\mathbf{C}}=\overline{\mathbf{F}}^T\overline{\mathbf{F}}=J^{-2/3}\mathbf{C},$$

and the first fiber invariant (2.12a) is given by

$$\overline{I}_4=\mathbf{A}^T\overline{\mathbf{C}}\mathbf{A}=J^{-2/3}I_4, \tag{3.9}$$

it follows from the proof of Theorem 1 that for motions satisfying (3.6), the invariant $\overline{I}_4$ *is only a function of J, and is thus not an independent invariant.*

4. Motions transverse to a plane

We consider the solutions of the partial differential equations (PDEs) (2.20) in the form of fully non-linear perturbations $\mathbf{G}(\mathbf{X},t)$ of the stress-free configuration, i.e.,

$$\mathbf{x}=\mathbf{X}+\mathbf{G}(\mathbf{X},t),$$

which must be compatible with the incompressibility condition (2.20a). Importantly, the ansätze considered below are not limited to linear or plane waves.

The first ansatz considered describes transverse displacements orthogonal to the (X^1,X^2) plane, and is referred to as *linearly polarized motions* in [8], and *anti-plane shear* in [33]. The coordinate dependence for such displacements is given by

$$\mathbf{x}=\begin{bmatrix}X^1\\ X^2\\ X^3+G\left(X^1,X^2,t\right)\end{bmatrix}. \tag{4.1}$$

See Fig. 1 for a sample deformation of this type. We consider the fiber family directed along a unit orientation vector in the reference configuration,

$$\mathbf{A}=\begin{bmatrix}\cos\gamma\\ 0\\ \sin\gamma\end{bmatrix}, \tag{4.2}$$

where $\gamma=\text{const}\in[0,\pi/2]$ is the angle with the direction X^1 in the (X^1,X^3)-plane. Thus generally, the displacements given by (4.1) do not have a special orientation with respect to the fiber family.

Since the deformation gradient for motions described by (4.1) takes the form

$$\mathbf{F}=\begin{bmatrix}1 & 0 & 0\\ 0 & 1 & 0\\ \partial G/\partial X_1 & \partial G/\partial X_2 & 1\end{bmatrix},$$

one has $J\equiv1$, and the incompressibility condition is identically satisfied.

Using the ansatz (4.1) in the dynamic equations (2.20), and denoting constants $\alpha=2(a+b)>0$ and $\beta=4q>0$, we obtain the three PDEs

$$\begin{aligned}\frac{\partial^2 G}{\partial t^2}=&\alpha\left(\frac{\partial^2 G}{\partial\left(X^1\right)^2}+\frac{\partial^2 G}{\partial\left(X^2\right)^2}\right)\\ &+\beta\cos^2(\gamma)\left(3\cos^2(\gamma)\left(\frac{\partial G}{\partial X^1}\right)^2+6\cos(\gamma)\sin(\gamma)\frac{\partial G}{\partial X^1}\right.\\ &\left.+2\sin^2\gamma\right)\frac{\partial^2 G}{\partial\left(X^1\right)^2},\end{aligned} \tag{4.3}$$

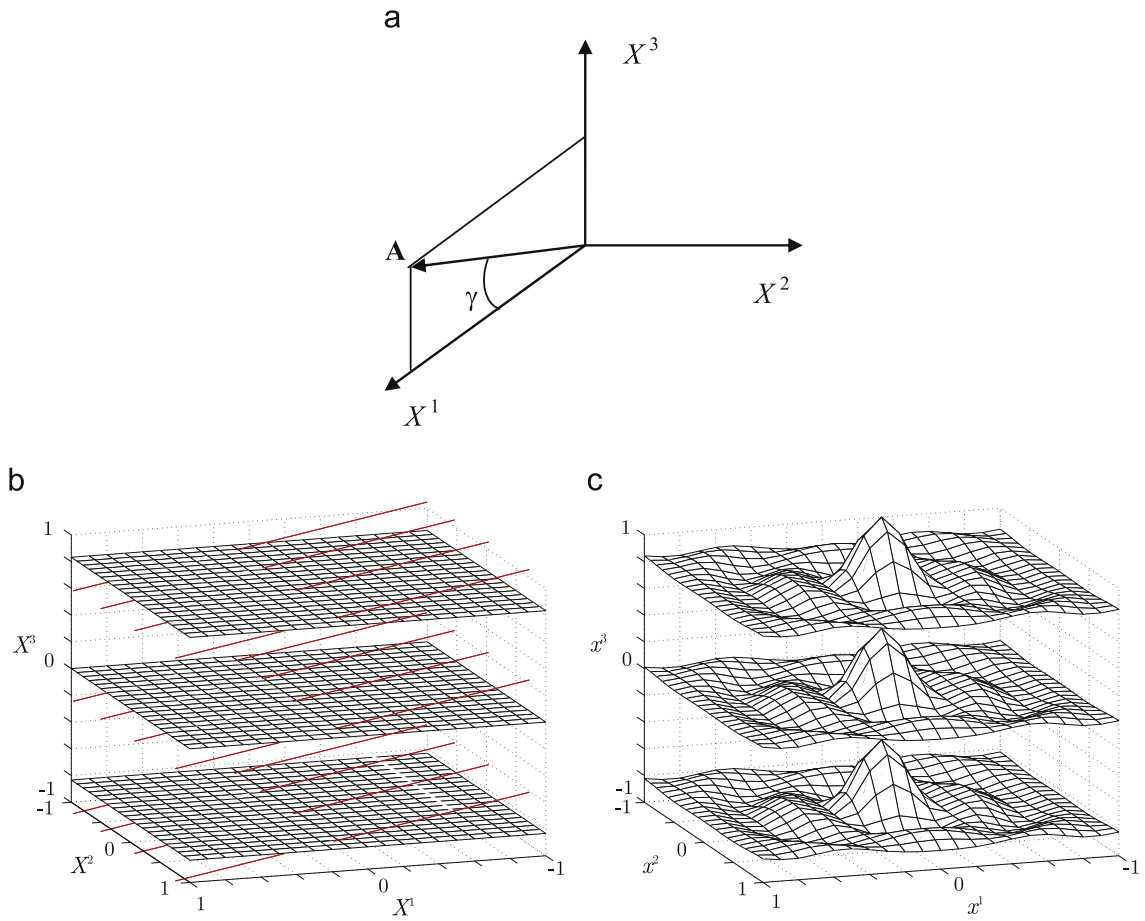

Fig. 1. (a) Fiber direction. (b) The reference (Lagrangian) mesh with fibers. (c) A sample deformed mesh (Eulerian configuration) for the ansatz (4.1).

$$0=\frac{\partial p}{\partial X^1}+2b\rho_0\left(\frac{\partial G}{\partial X^1}\frac{\partial^2 G}{\partial (X^2)^2}-\frac{\partial G}{\partial X^2}\frac{\partial^2 G}{\partial X^1\partial X^2}\right)$$
$$-2\beta\rho_0\cos^3\gamma\frac{\partial^2 G}{\partial (X^1)^2}\left(\cos\gamma\frac{\partial G}{\partial X^1}+\sin\gamma\right), \tag{4.4}$$

$$0=\frac{\partial p}{\partial X^2}+2b\rho_0\left(\frac{\partial G}{\partial X^2}\frac{\partial^2 G}{\partial (X^1)^2}-\frac{\partial G}{\partial X^1}\frac{\partial^2 G}{\partial X^1\partial X^2}\right), \tag{4.5}$$

for the two unknown functions $G\left(X^1,X^2,t\right)$ and $p\left(X^1,X^2,t\right)$. The PDEs (4.3)–(4.5) involve three constant material parameters: $a,b>0$ (the Mooney–Rivlin parameters) and $q>0$ (the fiber family parameter). The constant density ρ_0 can be eliminated by rescaling the pressure.

The PDEs (4.4) and (4.5) define the pressure p through its gradient if and only if the compatibility condition is satisfied:

$$\frac{\partial^2 p}{\partial X^1\partial X^2}=\frac{\partial^2 p}{\partial X^2\partial X^1},$$

which takes the form of a differential constraint on the displacement:

$$b\frac{\partial}{\partial X^1}\left[\frac{\partial G}{\partial X^1}\frac{\partial^2 G}{\partial X^1\partial X^2}-\frac{\partial G}{\partial X^2}\frac{\partial^2 G}{\partial (X^1)^2}\right]$$
$$=\frac{\partial}{\partial X^2}\left[\beta\cos^3\gamma\frac{\partial^2 G}{\partial (X^1)^2}\left(\cos\gamma\frac{\partial G}{\partial X^1}+\sin\gamma\right)\right.$$
$$\left.+b\left(\frac{\partial G}{\partial X^2}\frac{\partial^2 G}{\partial X^1\partial X^2}-\frac{\partial G}{\partial X^1}\frac{\partial^2 G}{\partial (X^2)^2}\right)\right]. \tag{4.6}$$

The displacement $G(X^1,X^2,t)$ thus must satisfy the overdetermined system of two PDEs given by (4.3) and (4.6).

Special cases of 1+1-dimensional non-linear motions in X^1- and X^2- directions are considered in Sections 4.2 and 4.3.

Remark 3. Overdetermined PDE systems similar to (4.3) and (4.6) arise for incompressible anti-plane shear deformations (4.1) for any form of the strain energy density W. The classification problem of determining the forms of strain energy density which admit non-trivial states of anti-plane shear, that is, for which the compatibility constraint is identically satisfied for every solution $G(X^1,X^2,t)$, has been considered from different viewpoints, and in different physical settings. (See, e.g., [21,25,47] and references therein.) To our knowledge, however, no similar results are available concerning the anisotropic strain energy density forms used in this work (Section 2.2).

4.1. Symmetry classification of the non-linear two-dimensional PDE system (4.3) and (4.6)

We now seek Lie groups of point transformations admitted by the PDEs (4.3) and (4.6), in the form

$$G^*=g(X^1,X^2,t,G;\varepsilon)=G+\varepsilon\eta(X^1,X^2,t,G)+O(\varepsilon^2),$$
$$(X^*)^i=f^i(X^1,X^2,t,G;\varepsilon)=z^i+\varepsilon\xi^i(X^1,X^2,t,G)+O(\varepsilon^2),\quad i=1,2,$$
$$t^*=h(X^1,X^2,t,G;\varepsilon)=u^\mu+\varepsilon\tau(X^1,X^2,t,G)+O(\varepsilon^2), \tag{4.7}$$

involving the group parameter ε. Generalizations of point transformations including higher-order and non-local symmetries are available but are out of scope of this paper.

The computation of the Lie group of admissible transformations (4.7) is equivalent to finding the Lie algebra *infinitesimal*

Table 1
Lie point symmetry classification for Theorem 2.

Parameters	Symmetries
Arbitrary	$Y^1=\frac{\partial}{\partial t}$, $Y^2=\frac{\partial}{\partial X^1}$, $Y^3=\frac{\partial}{\partial X^2}$, $Y^4=\frac{\partial}{\partial G}$, $Y^5=t\frac{\partial}{\partial G}$, $Y^6=X^1\frac{\partial}{\partial X^1}+X^2\frac{\partial}{\partial X^2}+t\frac{\partial}{\partial t}+G\frac{\partial}{\partial G}$
$\gamma=\pi/2$ or $\beta\equiv 4q=0$	Y^1, Y^2, Y^3, Y^4, Y^5, Y^6, $Y^7=-X^2\frac{\partial}{\partial X^1}+X^1\frac{\partial}{\partial X^2}$, $Y^8=G\frac{\partial}{\partial G}$

generators (tangent vector fields)

$$Y=\xi^i(X^1,X^2,t,G)\frac{\partial}{\partial X^i}+\tau(X^1,X^2,t,G)\frac{\partial}{\partial t}+\eta(X^1,X^2,t,G)\frac{\partial}{\partial G}. \tag{4.8}$$

The application of Lie algorithm to the PDEs (4.3) and (4.6), and a classification of symmetries according to the constitutive parameters, yields the following result.

Theorem 2. *The classification of point symmetries of the PDE system (4.3) and (4.6) of motions of a non-linear two-dimensional elastic material perpendicular to a plane is given in Table 1.*

The symmetries Y^1 to Y^4 correspond to space and time translations; Y^5 is the Galilean group in the direction of displacement; Y^6 is a homogeneous space–time scaling.

The special case arises in the symmetry classification when $q\cos\gamma=0$, i.e., fibers are absent, or the fiber bundle is perpendicular to the X^1 X^2-plane, which turns out to be equivalent to the isotropic Mooney–Rivlin model with no fibers present. This is in agreement with Theorem 1. The symmetries Y^7 (rotation) and Y^8 (scaling of G) arise in this special case due to its extra geometrical symmetry. In particular, the PDEs (4.3) and (4.6) become

$$\frac{\partial^2 G}{\partial t^2}=\alpha\left(\frac{\partial^2 G}{\partial\left(X^1\right)^2}+\frac{\partial^2 G}{\partial\left(X^2\right)^2}\right),b\left\{\frac{\partial}{\partial X^1}\left[\frac{\partial G}{\partial X^2}\left(\frac{\partial^2 G}{\partial (X^1)^2}+\frac{\partial^2 G}{\partial (X^2)^2}\right)\right]\right.$$
$$\left.+\frac{\partial}{\partial X^2}\left[\frac{\partial G}{\partial X^1}\left(\frac{\partial^2 G}{\partial (X^1)^2}+\frac{\partial^2 G}{\partial (X^2)^2}\right)\right]\right\}=0,$$

i.e., a linear wave equation appended by a symmetric non-linear differential constraint. Due to the non-linear constraint, the system does not admit infinite symmetries natural to linear PDEs, unless $b=0$.

4.2. One-dimensional wave propagation (vertical displacement) independent of the fiber direction

Consider a special case of the general PDE system (4.3) and (4.6), when the displacement only depends on the direction X^2, and the fiber direction γ is arbitrary. The motion in the vertical direction is then described by

$$\mathbf{x}=\begin{bmatrix}X^1\\ X^2\\ X^3+Q\left(X^2,t\right)\end{bmatrix}. \tag{4.9}$$

Here the displacements project *non-trivially* on the fiber direction, in particular, the angle between the displacement direction and the fibers equals $\pi/2-\gamma$. The hydrostatic pressure is assumed to have the form $p=p(X^1,X^2,t)$. The following result holds.

Theorem 3. *For the fully non-linear anisotropic model of a hyperelastic fiber-reinforced material the constitutive law (2.22), equations governing finite one-dimensional displacements of the form (4.9) are linear; they are given by*

$$\frac{\partial^2 Q}{\partial t^2}=\alpha\frac{\partial^2 Q}{\partial (X^2)},\quad \frac{\partial P}{\partial X^1}=\frac{\partial P}{\partial X^2}=0. \tag{4.10}$$

In this case, for any fiber direction given by the angle γ in the (X^1,X^3)-plane, the displacement is independent of the fiber direction. Consequently, Theorem 1 holds, and the motion will not be influenced by the fibers.

Remark 4. Generally one might assume a more general dependence of the hydrostatic pressure, $p=p(X^1,X^2,X^3,t)$. One can show that in such a case, the pressure is at most linear in X^3:

$$p=p_1(t)(X^3+Q(X^2,t))+p_2(t),$$

and the PDE (4.10) has an extra forcing term $-p_1(t)$ on the right-hand side.

4.3. One-dimensional S-wave propagation dependent on the fiber direction

We now consider the second one-dimensional reduction of (4.1), where the displacement $G(X^1,t)$ of the solid from equilibrium along the X^3-axis is described by

$$\mathbf{X}=\begin{bmatrix}X^1\\ X^2\\ X^3+G\left(X^1,t\right)\end{bmatrix}; \tag{4.11}$$

this corresponds to motions in the fiber plane of X^1 X^3, perpendicular to the X^1 X^2-plane. The hydrostatic pressure is given by $p=p(X^1,t)$. The incompressibility condition is identically satisfied.

For simplicity of notation, within this subsection, we denote $X^1=x$ and use the subscript notation for derivatives. Accordingly, the equations of motion (4.3)–(4.5) simplify to

$$G_{tt}=\left(\alpha+\beta\cos^2\gamma\left[(3\cos^2\gamma)(G_x)^2+(6\sin\gamma\cos\gamma)G_x+2\sin^2\gamma\right]\right)G_{xx}, \tag{4.12}$$

$$0=p_x-2\beta\rho_0\cos^3\gamma(\cos\gamma G_x+\sin\gamma)G_{xx}, \tag{4.13}$$

where $G=G(x,t)$ and $p=p(x,t)$. The second PDE (4.13) yields an explicit form of the pressure

$$p=\beta\rho_0\cos^3\gamma(\cos\gamma G_x+2\sin\gamma)G_x+f(t), \tag{4.14}$$

in terms of the displacement G, for an arbitrary $f(t)$.

It is clear that since the Mooney–Rivlin parameter b does not appear in the PDEs (4.12) and (4.13) independently of the neo-Hookean parameter a, the model is equivalent to a purely neo-Hookean model depending on the parameter α.

Symmetry classification of the non-linear one-dimensional PDE (4.12), and its applications to finding exact solutions, is considered in the following section.

4.3.1. The hyperbolicity condition

We now consider the possibility of the loss of hyperbolicity in the PDE (4.12), which may lead to singular solution behavior. This can happen when the coefficient of G_{xx} vanishes and/or changes sign. This coefficient

$$\mathcal{C} = \alpha + \beta \cos^2\gamma \left(3\cos^2\gamma (G_x)^2 + 6\sin\gamma\cos\gamma G_x + 2\sin^2\gamma\right) = 0, \tag{4.15}$$

is a quadratic expression in G_x, and has real roots when the discriminant is non-negative, i.e.,

$$-3\beta(\alpha - \beta\sin^2\gamma\cos^2\gamma)) \geq 0,$$

or

$$\sin^2(2\gamma) \geq \frac{4\alpha}{\beta}. \tag{4.16}$$

The following result is established.

Lemma 1. *The one-dimensional PDE (4.12) is hyperbolic for any fiber orientation angle γ for all times, provided that*

$$4\alpha > \beta. \tag{4.17}$$

A necessary condition of the loss of hyperbolicity is that $4\alpha < \beta$, and that the fiber orientation angle γ satisfies (4.16).

In particular, if the fiber effects encoded by the material parameter β are small, equation (4.17) is always satisfied.

When the fiber effects are small, the sufficient condition of hyperbolicity (4.17) is always satisfied. Considering, for example, experimentally determined values of the constitutive parameters a, b, q can be adapted from [22] for the model (2.15) of the rabbit artery, one would have $a \sim 1.5$ kPa, $q \sim 1.18$ kPa for the artery media layer, and $a \sim 0.15$ kPa, $q \sim 0.28$ kPa for the adventitia layer. (In that model, $b \equiv 0$.) In both of the listed cases, $4\alpha/\beta > 1$, and the additional symmetry does not arise for any fiber orientation.

4.4. Symmetry classification and exact solutions of the one-dimensional wave propagation model (4.12)

We now classify Lie point symmetries in the local form

$$\mathrm{Z} = \xi(x,t,G)\frac{\partial}{\partial x} + \tau(x,t,G)\frac{\partial}{\partial t} + \eta(x,t,G)\frac{\partial}{\partial G} \tag{4.18}$$

of one-dimensional equation (4.12) for an arbitrary fiber direction $\gamma \neq 0, \pi/2$, assuming the non-triviality of material parameters: $\alpha, \beta > 0$. The following theorem is proven by direct computation.

Theorem 4. *The classification of point symmetries of the non-linear PDE (4.12) with respect to the parameters $\gamma \neq 0, \pi/2$, $\alpha > 0$, $\beta > 0$ is given in Table 2.*

A special "shear" symmetry group given by the generator Z^6 arises in the case of the special fiber orientation (4.16).

Symmetries $\mathrm{Z}^1, \mathrm{Z}^2, \mathrm{Z}^3$ correspond to time and space translations; Z^4 is the Galilean group in the direction of displacement; Z^5 is the space–time scaling.

Table 2
Lie point symmetry classification for Theorem 4.

Parameters	Symmetries
Arbitrary	$\mathrm{Z}^1 = \frac{\partial}{\partial x}$, $\mathrm{Z}^2 = \frac{\partial}{\partial t}$, $\mathrm{Z}^3 = \frac{\partial}{\partial G}$, $\mathrm{Z}^4 = t\frac{\partial}{\partial G}$, $\mathrm{Z}^5 = x\frac{\partial}{\partial x} + t\frac{\partial}{\partial t} + G\frac{\partial}{\partial G}$
$4\alpha \leq \beta$, $\sin^2 2\gamma = \frac{4\alpha}{\beta}$	Z^1, Z^2, Z^3, Z^4, Z^5, $\mathrm{Z}^6 = 2t\cos\gamma\frac{\partial}{\partial t} + x\cos\gamma\frac{\partial}{\partial x} - x\sin\gamma\frac{\partial}{\partial G}$

The global form of point transformations corresponding to the special group Z^6 has the form

$$t^* = e^{2\varepsilon}\, t, \quad x^* = e^{\varepsilon}\, x, \quad G^* = G + \tan\gamma(1 - e^{\varepsilon})x. \tag{4.19}$$

In particular, transformations (4.19) map the equilibrium solution $G = 0$ corresponding to the unperturbed medium with $x^{1,2,3} = X^{1,2,3}$, $p = \text{const}$ into shear equilibrium solutions

$$x^1 = X^1, \quad x^2 = X^2, \quad x^3 = X^3 + AX^1, \quad A = \text{const}.$$

Remark 5. We note that the angle γ between the fiber orientation and the wave propagation direction giving rise to the special symmetry group given by Z^6 satisfies the necessary (but not sufficient!) condition of the loss of hyperbolicity (4.16):

$$\sin^2 2\gamma = \frac{4\alpha}{\beta}. \tag{4.20}$$

For specific solutions, the coefficient (4.15) may or may not actually vanish. An example of an exact solution in a situation when (4.20) is satisfied but the wave equation remains hyperbolic for all times is given in Section 4.4.2.

4.4.1. Contact symmetries and linearization

Similar to Lie point symmetries, one may seek contact symmetries (e.g., [4])

$$\hat{Z} = \zeta(x,t,G,\partial G)\frac{\partial}{\partial G}. \tag{4.21}$$

As it is well-known, PDEs for $u(x,t)$ of the form

$$A(u_x,u_t)u_{tt} + B(u_x,u_t)u_{xt} + C(u_x,u_t)u_{xx} = 0 \tag{4.22}$$

admit an infinite number of contact symmetries. The one-dimensional wave propagation model (4.12) has contact symmetries (4.21) with components $\zeta(G_x, G_t)$ satisfying a linear PDE

$$\zeta_{G_x,G_x} = \left[\alpha + \beta\cos^2\gamma\left[(3\cos^2\gamma)G_x^2 + (6\sin\gamma\cos\gamma)G_x + 2\sin^2\gamma\right]\right]\zeta_{G_t,G_t} \tag{4.23}$$

It follows (see, for example, [4]) that the non-linear wave equation (4.12) can be invertibly mapped into a linear wave equation by a Legendre contact transformation

$$u = G_x, \quad v = G_t, \quad W(u,v) = G(x,t) - xG_x - tG_t.$$

The corresponding linear wave equation is given by

$$W_{uu} = \left[\alpha + \beta\cos^2\gamma\left[(3\cos^2\gamma)u^2 + (6\sin\gamma\cos\gamma)u + 2\sin^2\gamma\right]\right]W_{vv}.$$

We also note that the non-linear wave equation (4.12) can be linearized by a *non-local* hodograph transformation (cf. [4]).

4.4.2. An example of an exact invariant solution

We now study the invariant reduction of the PDE (4.12) under the special symmetry Z^6, in the case of the special fiber orientation satisfying (4.20). The two invariants of the symmetry Z^6 can be chosen, for example, to be

$$y = \frac{x}{\sqrt{t}}, \quad M(y) = \sqrt{12\beta}\cos^2\gamma(G(x,t) + x\tan\gamma). \tag{4.24}$$

In terms of the invariants (4.24), the reduced equation is a second-order ODE

$$M''(y) = \frac{3M'(y)}{(M'(y))^2 - y^2}, \tag{4.25}$$

which is further reducible to a first-order ODE, but does not admit a general solution in terms of elementary functions. The ODE (4.25) is invariant under reflections $y \to -y$ and under translations $M \to M + \text{const}$. Sample solutions of Eq. (4.25) can be obtained numerically. As an example, we compute the dimensionless solution of the ODE

(4.25) with initial conditions

$$M(0)=0, \quad M'(0)=m_0.$$

Asymptotically, for any $m_0>0$, $M\to y|y|$ as $|y|\to\infty$. We choose $m_0=1$. Using the time-translation symmetry Z^2, the corresponding physical solution found from (4.24) can be written as

$$G(x,t)=\frac{1}{\sqrt{12\beta}\cos^2\gamma}M\left(\frac{x}{\sqrt{t+t_0}}\right)-x\tan\gamma, \quad t_0=\text{const}. \tag{4.26}$$

The solutions (4.26) represent the degeneration of the parabolic shear to the simple linear shear solution $G=-x\tan\gamma$ as $t\to\infty$.

In Fig. 2, sample dimensionless solutions (4.26) are plotted as functions of x for $\gamma=\pm\pi/4$, $\alpha=1/12$, $\beta=1/3$, $m_0=1$, and times $t=0,2,5,20$. The coefficient $\mathcal{C}$ (4.15) are also shown as functions of x,t; it is clear that they remain positive, and the loss of hyperbolicity of the non-linear wave equation does not occur for this solution. In general, for solutions (4.26), one has

$$\mathcal{C}(x,t)=\frac{1}{4(t+1)}M'\left(\frac{x}{\sqrt{t+t_0}}\right), \quad \min_x \mathcal{C}(x,t)=\mathcal{C}(0,t)=\frac{m_0}{4(t+t_0)}, \tag{4.27}$$

the latter being strictly positive for the indicated parameters, independently of the sign of $\gamma=\pm\pi/4$.

4.5. Special fiber orientations

We now consider specific cases of Eq. (4.12) for special fiber orientations.

4.5.1. Case 1: $\gamma=\pi/2$

When the fibers are directed along X^3, i.e., $\gamma=\pi/2$, the displacement $G(x,t)$ is independent of the fiber direction. As a result, according to Theorem 1, the fiber-dependent terms in the dynamic equation vanish. Indeed, PDEs (4.12) and (4.13) yield a

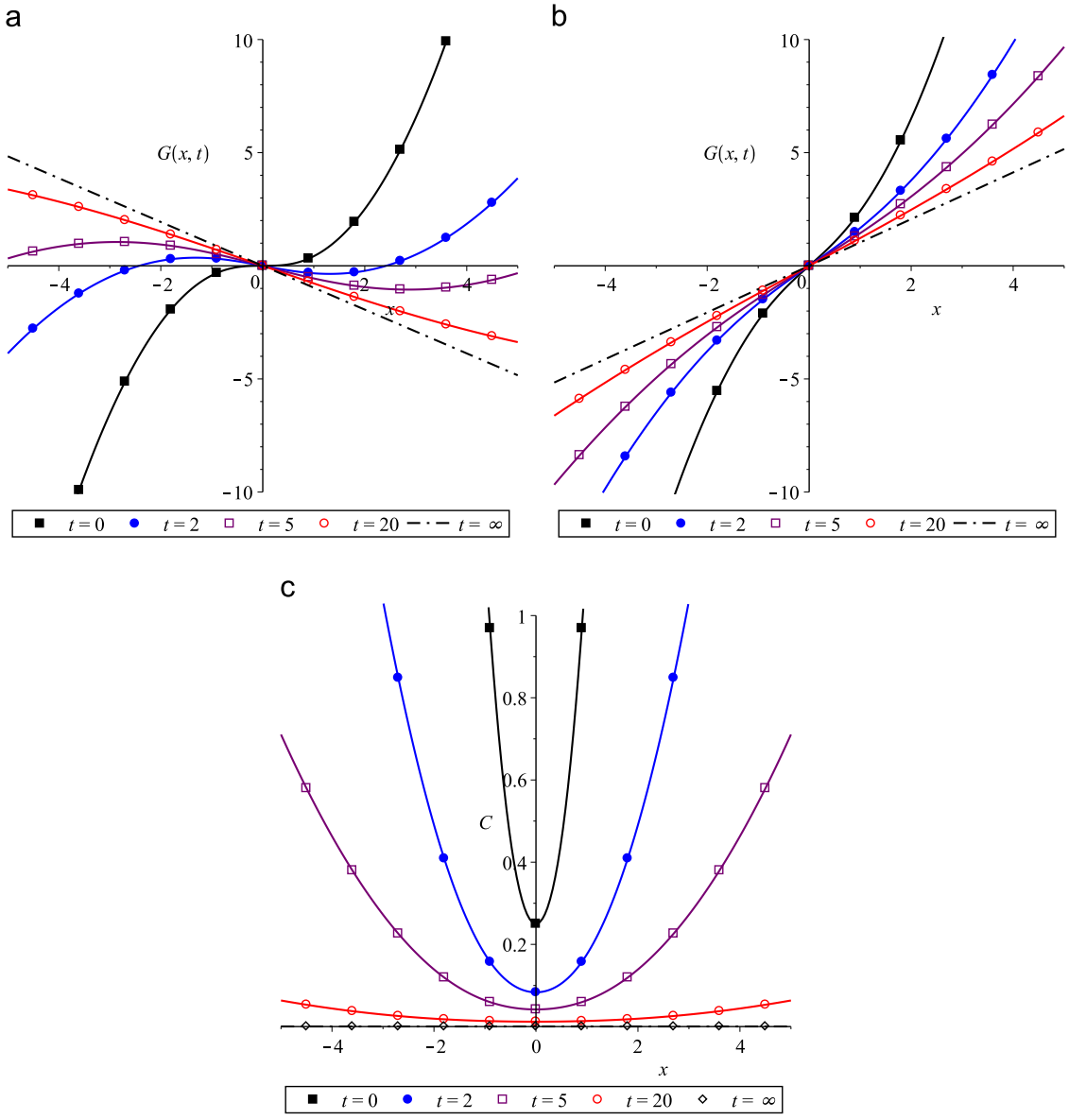

Fig. 2. (a) Sample dimensionless solutions (4.26) as functions of x for $\alpha=1/12$, $\beta=1/3$, $m_0=1$, $\gamma=\pi/4$, at times $t=0,2,5,20$. (b) The same plots for $\gamma=-\pi/4$. (c) The corresponding plots of the wave equation coefficient $\mathcal{C}$ (4.15) and (4.27).

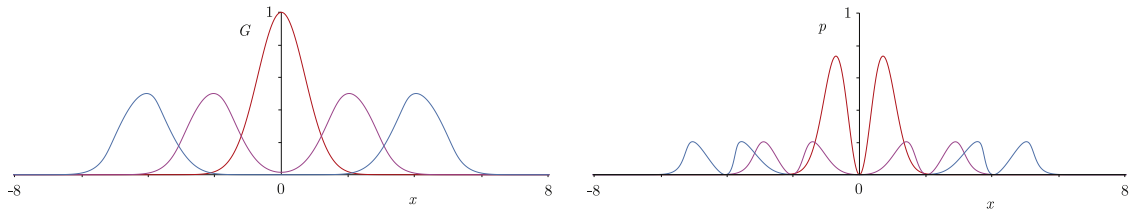

Fig. 3. Plot of numerical solution of the PDEs (4.14) and (4.28) for $\alpha=1$, $\beta=1/3$, $\rho_0=1$, with initial conditions (4.29). The colors red, magenta, and blue correspond to the solution at times $t=0,2,4$, respectively. (For interpretation of the references to color in this figure caption, the reader is referred to the web version of this paper.)

linear wave equation

$$G_{tt}=\alpha G_{xx},\quad p_x=0.$$

4.5.2. Case 2: $\gamma=0$

In an opposite case, when the fibers are directed along X^1, the displacement $G(x,t)$ is orthogonal to fibers but propagates in the fiber direction. The dynamic equation (4.12) reduces to a non-linear wave equation

$$G_{tt}=\left(\alpha+3\beta(G_x)^2\right)G_{xx}. \tag{4.28}$$

We are not aware of physically non-trivial closed-form solutions of the PDE (4.28); in particular, it does not admit traveling wave solutions of physical interest. We numerically compute a d'Alembert-type numerical solution for the initial value problem consisting of the PDE (4.28) with the initial conditions

$$G(x,0)=u_0(x),\quad G_t(x,0)=0,\quad x\in\mathbb{R}, \tag{4.29}$$

and the asymptotic requirement $G(x,t)\to 0$ as $|x|\to\infty$. Without loss of generality, if $\alpha,\beta\neq 1$, Eqs. (4.14) and (4.28) can be re-scaled into a dimensionless form with $\alpha=3\beta=\rho_0=1$. For a specific initial condition

$$u_0(x)=\exp(-x^2),$$

the evolution of the wave form for $G(x,t)$ and $p(x,t)=(1/3)G_x$ is shown in Fig. 3. The evolution is symmetric under the reflection $x\to x$ since this symmetry of the equation is respected by the initial conditions. Unlike the classical d'Alembert solution for the linear wave equation, in the non-linear situation, the shape of the moving waves is not time-invariant, which may lead to wave breaking. Indeed, for the wave speed, one has $c^2=\alpha 3\beta G x^2$, i.e., the points on the solution curve corresponding to higher values of the curve slope $|Gx|$ move faster, which results in a shock formation. Such non-physical behavior is a result of exceeding the physical applicability limits of the incompressible non-dissipative model. A similar phenomenon of shock formation has been observed in [39], where a generalization of Carroll's circularly polarized wave solutions [8] is developed.

5. Motions transverse to an axis

5.1. The non-linear equations for general and specific fiber orientations

We now study another class of displacements for which the incompressibility condition is identically satisfied: the motions transverse to the axis of X^1, given by

$$\mathbf{X}=\begin{bmatrix} X^1 \\ X^2+H\left(X^1,t\right) \\ X^3+G\left(X^1,t\right)\end{bmatrix}. \tag{5.1}$$

The hydrostatic pressure p is assumed to have the form $p=p(X^1,t)$. The fibers are oriented along the unit vector (4.2) in the same manner as earlier, without a loss of generality. We again denote $X^1=x$ for simplicity of notation, and use the subscript notation for derivatives.

Combining the ansatz (5.1) with the dynamic equations (2.20), one arrives at the three PDEs

$$0=p_x-2\beta\rho_0\cos^3\gamma[(\cos\gamma G_x+\sin\gamma)G_{xx}+\cos\gamma H_xH_{xx}], \tag{5.2}$$

$$H_{tt}=\alpha H_{xx}+\beta\cos^3\gamma\left[\cos\gamma([G_x^2+H_x^2]H_{xx}+2G_xH_xG_{xx})+2\sin\gamma\frac{\partial}{\partial x}(G_xH_x)\right], \tag{5.3}$$

$$G_{tt}=\alpha G_{xx}+\beta\cos^2\gamma\left[2\sin^2\gamma\ G_{xx}+\cos^2\gamma\left(2G_xH_xH_{xx}+\left(H_x^2+3G_x^2\right)G_{xx}\right)+\sin 2\gamma(3G_xG_{xx}+H_xH_{xx})\right], \tag{5.4}$$

where again $\alpha=2(a+b)>0$, and $\beta=4q>0$.

It is clear that the model (5.2)–(5.4) reduces directly to the one-dimensional PDE system (4.12)–(4.13) when $H=0$.

Eq. (5.2) again yields an exact general solution for the pressure as

$$p=\beta\rho_0\cos^3\gamma\left[\cos\gamma\ (G_x^2+H_x^2)+2\sin\gamma\ G_x\right]+f(t), \tag{5.5}$$

and the two PDEs (5.3) and (5.4) are pressure-independent.

We note that the PDEs (5.3) and (5.4) can be written in the conserved form

$$H_{tt}=\frac{\partial}{\partial x}\left(\left[\alpha+\beta\cos^3\gamma\left\{(G_x^2+H_x^2)\cos\ \gamma+2G_x\sin\gamma\right\}\right]H_x\right), \tag{5.6}$$

$$G_{tt}=\frac{\partial}{\partial x}\left(\alpha G_x+\beta\cos^2\gamma\left[2\sin^2\gamma\ G_x\ +\cos^2\gamma(G_x^2+H_x^2)G_x+\sin\gamma\cos\gamma(3G_x^2+H_x^2)\right]\right). \tag{5.7}$$

We now consider the simplifications of these PDEs for specific fiber orientations.

5.1.1. Special case 1: $\gamma=\pi/2$

When the fibers are directed along X^3, both displacements $H(x,t)$, $G(x,t)$ are independent of the fiber direction. In agreement with Theorem 1, such motions are described by independent linear PDEs

$$H_{tt}=\alpha H_{xx},\quad G_{tt}=\alpha G_{xx}, \tag{5.8}$$

with multiple exact solutions available through standard methods.

5.1.2. Special case 2: $\gamma=0$

When the fibers are directed along $X^1=x$, the displacement is orthogonal to fibers and propagates in the fiber direction. The dynamic equations describing such motions are symmetric, and are given by

$$H_{tt}=\frac{\partial}{\partial x}\left(\alpha+\beta\left(G_x^2+H_x^2\right)H_x\right),\quad G_{tt}=\frac{\partial}{\partial x}\left(\alpha+\beta\left(G_x^2+H_x^2\right)G_x\right), \tag{5.9}$$

with the non-linear terms describing the effect of fibers.

Table 3
Lie point symmetry classification for Theorem 5.

Parameters	Symmetries
Arbitrary	$W^1=\frac{\partial}{\partial x}$, $W^2=\frac{\partial}{\partial t}$, $W^3=\frac{\partial}{\partial H}$, $W^4=\frac{\partial}{\partial G}$, $W^5=t\frac{\partial}{\partial H}$, $W^6=t\frac{\partial}{\partial W}$, $W^7=x\frac{\partial}{\partial x}+t\frac{\partial}{\partial t}+H\frac{\partial}{\partial H}+G\frac{\partial}{\partial G}$, $W^8=\cos\gamma\left(H\frac{\partial}{\partial G}-G\frac{\partial}{\partial H}\right)-x\sin\gamma\frac{\partial}{\partial H}$
$4\alpha\le\beta$, $\sin^2 2\gamma=\frac{4\alpha}{\beta}$	W^1, W^2, W^3, W^4, W^5, W^6, W^7, W^8, $W^9=2t\cos\gamma\frac{\partial}{\partial t}+x\cos\gamma\frac{\partial}{\partial x}-x\sin\gamma\frac{\partial}{\partial G}$

5.2. Point symmetry analysis

We now classify the Lie point symmetries

$$W=\xi(x,t,H,G)\frac{\partial}{\partial x}+\tau(x,t,H,G)\frac{\partial}{\partial t}+\eta(x,t,H,G)\frac{\partial}{\partial H}+\zeta(x,t,H,G)\frac{\partial}{\partial G}$$

of the PDEs (5.3)–(5.4) in the fully non-linear case.

Theorem 5. *The Lie point symmetry classification of the system (5.3)–(5.4) for material parameters $\alpha>0$, $\beta>0$, and the fiber angle $\gamma\in[0,\pi/2)$ is given in Table 3.*

The proof follows from the application of Lie's algorithm.

Similar to the case of one-dimensional perturbations studied in Table 2, a special symmetry W^9 arises when the angle γ between the fiber bundle and the wave propagation direction satisfies (4.20).

The other symmetries additional to the one-dimensional case of Table 2, holding for an arbitrary set of material parameters, are the Galilean group W^5 in the x^2-direction, and the fiber-dependent rotation group W^8. The latter has the global form

$$\begin{aligned}&t^*=t,\quad x^*=x,\\&H^*=H\cos\phi+G\sin\phi+x\tan\gamma\sin\phi,\\&G^*=-H\sin\phi+G\cos\phi-x\tan\gamma(1-\cos\phi),\end{aligned}\tag{5.10}$$

where ϕ is the group parameter. The transformations (5.10) reduce to a usual rotation group when $\gamma=0$, and to the shear transformation

$$t^*=t,\quad x^*=x,\quad H^*=H+\phi x,\quad G^*=G$$

when $\gamma=\pi/2$.

5.3. Exact solutions in the traveling wave ansatz

We are now interested in using the traveling wave ansatz to seek exact solutions of Eqs. (5.3) and (5.4). Traveling wave solutions will exist due to the presence of the traveling wave symmetry

$$W_{tw}=c\frac{\partial}{\partial x}+\frac{\partial}{\partial t},$$

holding for an arbitrary constant c. The invariants of W_{tw} are given by

$$r=x-ct,\quad H(x,t)=h(r),\quad G(x,t)=g(r).$$

Using the specified ansatz, we obtain the balance of momentum equations in the form of two ODEs

$$\begin{aligned}&\left[\alpha-c^2+\beta\cos^4\gamma(3(h')^2+(g')^2)+2\beta\sin\gamma g'\right]h''+2\beta\cos^3\gamma[\cos\gamma\, g'\\&\quad+\sin\gamma]h'g''=0,\quad 2\beta\cos^3\gamma[\cos\gamma\, g'+\sin\gamma]h'h''+[\alpha-c^2+\beta\cos^2\gamma\\&\quad\times\left(\cos^2\gamma\,[(h')^2+3(g')^2]+3\sin 2\gamma\, g'+2\sin^2\gamma\right)]g''=0,\end{aligned}\tag{5.11}$$

where the prime denotes differentiation d/dr.

Exact solutions can be constructed for the ODEs (5.11). We give an example of such solutions when the fibers are directed along the axis of x, i.e., $\gamma=0$. Eq. (5.11) simplifies to a symmetric form

$$\begin{aligned}&\left[\alpha-c^2+\beta(3(h')^2+(g')^2)\right]h''+2\beta g'h'g''=0,\\&2\beta g'h'h''+\left[\alpha-c^2+\beta((h')^2+3(g')^2)\right]g''=0.\end{aligned}\tag{5.12}$$

The following theorem is proven by a direct computation.

Theorem 6. *An infinite-dimensional family of solutions of the system (5.12) arises from an arbitrary pair of functions $g(r), h(r)$ satisfying an ODE*

$$(g')^2+(h')^2=R^2,\tag{5.13}$$

where

$$R^2=\frac{c^2-\alpha}{B}$$

is a dimensionless constant.

Thus any two functions whose slopes satisfy the equation of a circle (5.13) yield a traveling wave solution of the elasticity model (5.3) and (5.4). For the solution to be non-trivial, the speed c at which the deformation propagates must satisfy

$$c>c_0=\sqrt{\alpha}=\sqrt{2(a+b)}.$$

The deformations thus propagate at speeds greater than the wave speed c_0 of the linearized model. From the relation (5.13) it is evident that the *slopes* of the traveling perturbations must stay bounded.

We note that the relation (5.13) is the same as the one obtained by Carroll in [8] in a different context.

Example 1 (*A traveling shear wave*). Consider a Gaussian-shaped perturbation in the direction of X^3, given by

$$g(r)=\ell\exp(-r^2/\ell^2),\quad \ell>0.\tag{5.14}$$

For the perturbation in the direction of X^2, one obtains from (5.13),

$$h(r)=\int_0^r\sqrt{R^2-\frac{4s^2}{\ell^2}\exp(-2s^2/\ell^2)}\,ds.\tag{5.15}$$

It is straightforward to show that for any ℓ, as $|r|\to\infty$, the function $h(r)$ has an oblique asymptote

$$h(r)\to Rr.$$

The resulting solution of the elasticity equations, in the common notation of formula (5.1), has the form

$$G(x,t)=g(x-ct)=\ell\exp(-(x-ct)^2/\ell^2).\tag{5.16}$$

For the perturbation in the direction of X^2, one obtains from (5.13),

$$H(x,t)=h(x-ct)=\int_0^{x-ct}\sqrt{R^2-\frac{4s^2}{\ell^2}\exp(-2s^2/\ell^2)}\,ds.\tag{5.17}$$

The latter has the asymptotics $H(x,t)\sim R(x-ct)$ as $|x-ct|\to\infty$. Using the symmetry $W^5=t\partial/\partial H$ admitted by the model, one can remove the time-dependent part of the asymptotic behavior, taking

$$\tilde H(x,t)=H(x,t)+Rct.$$

The latter, for any t, has a time-independent asymptotics of a simple shear as $|x|\to\infty$:

$$\tilde H(x,t)\underset{|x|\to\infty}{\to}Rx.\tag{5.18}$$

As such, this can be written as

$$\tilde H(x,t)=Q(x,t)+Rx,\tag{5.19}$$

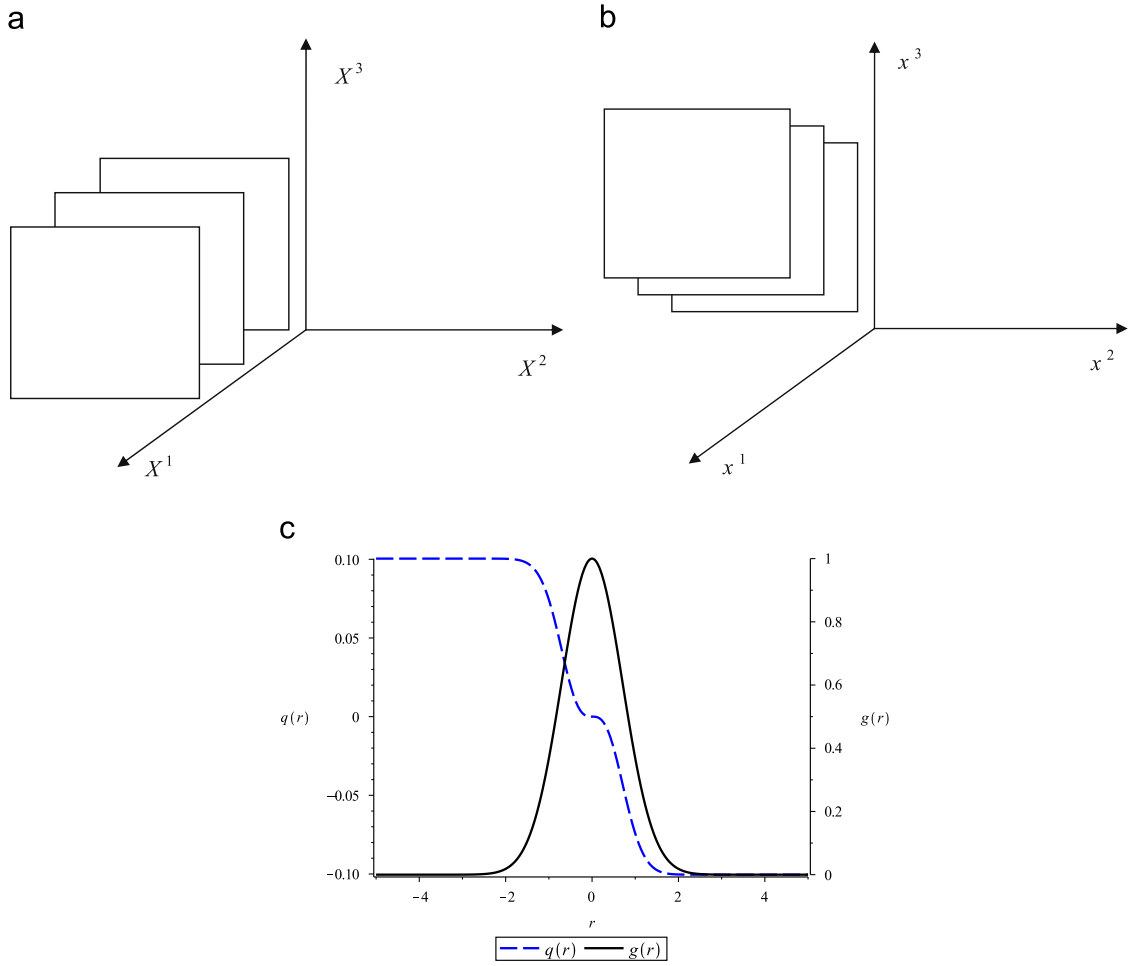

Fig. 4. Planes in the material frame (a), and a corresponding simple shear pre-strained configuration (5.21) in the actual frame (b). Traveling wave displacements (5.22) of the prestressed configuration (5.21) in the case of the fiber family oriented along the direction of X^1. Plots for $R=\sqrt{10}$, $\ell=1$ (c).

where

$$Q(x,t)=\int_0^{x-ct}\sqrt{R^2-\frac{4s^2}{\ell^2}\exp(-2s^2/\ell^2)}\,ds-R(x-ct)=q(r) \qquad (5.20)$$

is bounded for all x,t.

Fig. 4 shows the underlying pre-strained configuration

$$\mathbf{X}_0=\begin{bmatrix} X^1 \\ X^2+RX^1 \\ X^3 \end{bmatrix} \qquad (5.21)$$

and its traveling bounded perturbation

$$\mathbf{x}=\boldsymbol{\phi}(\mathbf{X},t)=\mathbf{X}_0+\begin{bmatrix} 0 \\ q(X^1-ct) \\ g(X^1-ct) \end{bmatrix} \qquad (5.22)$$

for a specific choice of parameters $R=\sqrt{10}$, $\ell=1$.

Example 2 (*A traveling periodic wave*). Another obvious solution of (5.13) is given by harmonic functions

$$h(r)=A\cos(kr+\phi_0),\quad g(r)=A\sin(kr+\phi_0),\quad A=R/k. \qquad (5.23)$$

This describes a time-periodic perturbation of the stress-free steady state, given by

$$\mathbf{x}=\boldsymbol{\phi}(\mathbf{X},t)=\begin{bmatrix} X^1 \\ X^2 \\ X^3 \end{bmatrix}+A\begin{bmatrix} 0 \\ \cos(k[X^1-ct]+\phi_0) \\ \sin(k[X^1-ct]+\phi_0) \end{bmatrix}. \qquad (5.24)$$

In this solution, every material point follows a circle. Material lines along the X^1 direction, given by $X^2=\text{const}$ and $X^3=\text{const}$, become helices parameterized by X^1 (Fig. 5). The solution therefore can be viewed as a *traveling helical shear wave.*

6. Conclusions

Anisotropy effects arising in various elastic materials due to the presence of a fibrous microstructure constitute an active research topic. Multiple models have been developed to account for the fiber effects; some of such models have been reviewed in Section 2. Due to the mathematical complexity of the underlying equations, a substantial part of the modern literature concerned with analysis and solution of anisotropic non-linear hyperelasticity models relies on the incremental analysis and the linearization of the governing equations. In this work, non-linear finite-amplitude displacement and wave propagation models in anisotropic hyperelastic Mooney–Rivlin-type materials were studied, assuming the presence of a single unidirectional

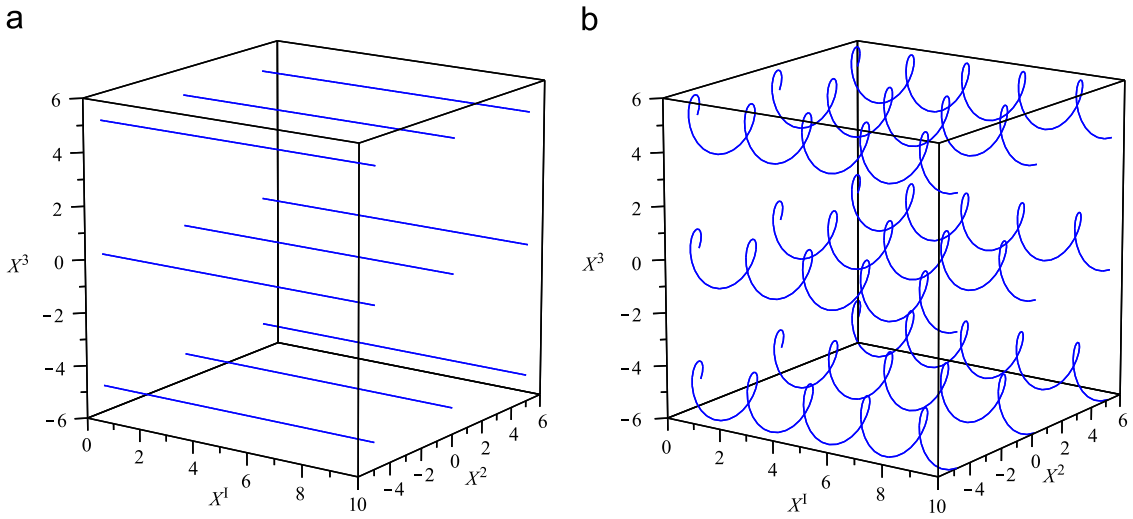

Fig. 5. Some material lines for $X^2 = \text{const}$, $X^3 = \text{const}$ in the reference configuration (a). The same lines in the actual configuration, parameterized by (5.24) (b).

family of fibers in the material configuration, following the standard reinforcing model (2.14).

For a general displacement pattern (3.3), a theorem proven in Section 4 states that for models involving the fiber contribution through the invariant I_4, displacements independent of the fiber direction do not depend on fiber effects. As such, a the well-known result from the incremental analysis framework has been generalized to the fully non-linear setting.

Section 4 considered anti-plane shear motions (4.1) for a general fiber orientation (4.2). A $2+1$-dimensional PDE system (4.3)–(4.5) describing the displacement and the hydrostatic pressure was derived. In particular, the displacement for such motions has been shown to satisfy a non-linear wave equation (4.3). The pressure compatibility condition led to Eq. (4.6), which effectively is a differential constraint on the displacement function, yielding an overdetermined PDE system. Lie point symmetries are classified with respect to constitutive parameters and fiber orientations. It was shown that displacements independent of the fiber direction, in the form (4.9), satisfy a linear wave equation (4.10), whereas the one-dimensional problem for the wave propagation with displacements dependent on the fiber direction yields a non-linear wave equation (4.12), essentially involving the fiber contribution. Even in the case of the fibers being orthogonal to the displacement, i.e., $\gamma=0$, one still has a non-linear wave equation (4.28). Sample numerical solutions of the latter were computed. The condition for the loss of hyperbolicity of the PDE (4.12) was derived. It was shown that when the fiber contribution is relatively small, the equation remains hyperbolic for all fiber orientations.

A special Lie point symmetry has been shown to exist for the considered model, in the one-dimensional setting (Section 4.4), and in the more general ansatz (5.1) in Section 5. The extra symmetry has the global form (4.19), and arises only in models with sufficiently strong fiber contribution, for specific mutual orientations of the wave vector and the fiber direction. For the one-dimensional model, the condition for the existence of the extra symmetry lies on the boundary of the domain of model parameters for which the loss of hyperbolicity of the PDE may occur. Exact solutions (4.26) invariant with respect to the special symmetry (4.19) describe the degeneration of a parabolic perturbation of a linearly pre-stressed two-dimensional configuration.

Traveling shear waves were considered in Section 5.3. From the motions of the form (5.1), general ordinary differential equations (5.11) for the displacements have been derived. In the computationally simpler case of perturbations propagating in the fiber direction, two families of exact solutions have been derived. The solution family (5.22) represents a bounded perturbation traveling along a pre-strained configuration. The second exact solution (5.24) describes a traveling helical shear wave. The solutions presented in Section 5.3 generalize Carrol's circularly polarized transverse waves for isotropic media [8].

The wave propagation equations and exact solutions derived in the current contribution for pre-strained and free elastic media are relevant to the description of waves in rubber-like fiber-reinforced materials, in both free and pre-stressed/pre-strained settings. In the future, it is planned to consider the more general situation of two families of fibers, which is necessary, for example, for an accurate description of soft biological tissues [22].

Other important directions of future work should include various realistic extensions of the considered constitutive model, such as models involving the fiber-dependent invariant I_5. For such models, motions with displacements independent of the fiber direction will generally be affected by fibers. Compressible models are also of interest; however, in multiple dimensions, such models are significantly more complicated due to the form of the barred invariants $\bar{I}_k$, $k=1,2,3\ldots$, which involve the non-constant Jacobian (see, e.g., [9]).

Acknowledgments

A.C. is grateful to NSERC of Canada for research support through a Discovery grant.

References

[1] C. Basciano, C. Kleinstreuer, Invariants-based anisotropic constitutive models of healthy aneurysmal abdominal aortic wall, J. Biomech. Eng. 131 (2009) 021009.
[2] S. Belkoff, R. Haut, A structural model used to evaluate the changing microstructure of maturing rat skin, J. Biomech. 24 (8) (1991) 711–720.
[3] M. Biot, Mechanics of Incremental Deformations, Wiley, New York, 1965.
[4] G. Bluman, A. Cheviakov, S. Anco, Applications of Symmetry Methods to Partial Differential Equations, Applied Mathematical Sciences, vol. 168, Springer, New York, 2010.
[5] G.W. Bluman, A.F. Cheviakov, S.C. Anco, Construction of conservation laws: how the direct method generalizes Noether's theorem, in: Proceedings of 4th Workshop in Group Analysis of Differential Equations & Integrability, 2009, pp. 1–23.
[6] G.W. Bluman, T. Temuerchaolu, Comparing symmetries and conservation laws of nonlinear telegraph equations, J. Math. Phys. 46 (7) (2005) 073513.
[7] P. Boulanger, M. Hayes, C. Trimarco, Finite-amplitude plane waves in deformed Hadamard elastic materials, Geophys. J. Int. 118 (2) (1994) 447–458.
[8] M.M. Carroll, Some results on finite amplitude elastic waves, Acta Mech. 3 (2) (1967) 167–181.

[9] A. Cheviakov, J.-F. Ganghoffer, Symmetry properties of two-dimensional Ciarlet–Mooney–Rivlin constitutive models in nonlinear elastodynamics, J. Math. Anal. Appl. 396 (2) (2012) 625–639.
[10] A.F. Cheviakov, GeM software package for computation of symmetries and conservation laws of differential equations, Comput. Phys. Commun. 176 (1) (2007) 48–61.
[11] P.G. Ciarlet, Mathematical Elasticity, Three-dimensional Elasticity, vol. 1, Collection Studies in Mathematics and Applications, vol. 20, Elsevier, Amsterdam, 1988.
[12] H. Demirkoparan, T. Pence, A. Wineman, Torsion of a fiber reinforced hyperelastic cylinder for which the fibers can undergo dissolution and reassembly, International Journal of Engineering Science 48 (11) (2010) 1179–1201.
[13] M. Destrade, A. Goriely, G. Saccomandi, Scalar evolution equations for shear waves in incompressible solids: a simple derivation of the Z, ZK, KZK and KP equations, Proc. R. Soc. A: Math. Phys. Eng. Sci. (2010) rspa20100508.
[14] M. Destrade, B. MacDonald, J. Murphy, G. Saccomandi, At least three invariants are necessary to model the mechanical response of incompressible, transversely isotropic materials, Comput. Mech. 52 (4) (2013) 959–969.
[15] M. Destrade, G. Saccomandi, Finite amplitude elastic waves propagating in compressible solids, Phys. Rev. E 72 (6) (2005) 016620.
[16] M. Destrade, G. Saccomandi, Creep, recovery, and waves in a nonlinear fiber-reinforced viscoelastic solid, SIAM J. Appl. Math. 68 (1) (2007) 80–97.
[17] M. Destrade, G. Saccomandi, I. Sgura, Inhomogeneous shear of orthotropic incompressible non-linearly elastic solids: singular solutions and biomechanical interpretation, Int. J. Eng. Sci. 47 (11) (2009) 1170–1181.
[18] Y.B. Fu, R.W. Ogden, Nonlinear Elasticity: Theory and Applications, Cambridge University Press, Cambridge, 2001.
[19] J. Hadamard, Leçons sur la Propagation des Ondes et les Equations de l'Hydrodynamique, Hermann, Paris, 1903.
[20] M. Hamilton, Y. Ilinski, A. Zabolotskaya, Separation of compressibility and shear deformation in the elastic energy density, J. Acoust. Soc. Am. 116 (2004) 41–44.
[21] J.M. Hill, Generalized shear deformations for isotropic incompressible hyperelastic materials, J. Aust. Math. Soc. Ser. B. Appl. Math. 20 (02) (1977) 129–141.
[22] G. Holzapfel, T. Gasser, R. Ogden, A new constitutive framework for arterial wall mechanics and a comparative study of material models, J. Elast. 61 (2000) 1–48.
[23] G. Holzapfel, R. Ogden, Constitutive modelling of arteries, Proc. R. Soc. A: Math. Phys. Eng. Sci. 466 (2010) 1551–1597.
[24] C. Horgan, G. Saccomandi, A new constitutive theory for fiber-reinforced incompressible nonlinearly elastic solids, J. Mech. Phys. Solids 53 (9) (2005) 1985–2015.
[25] J.K. Knowles, On finite anti-plane shear for incompressible elastic materials, J. Aust. Math. Soc. Ser. B. Appl. Math. 19 (04) (1976) 400–415.
[26] J.E. Marsden, T.J.R. Hughes, Mathematical Foundations of Elasticity, Dover, New York, 1994.
[27] J. Merodio, R.W. Ogden, Mechanical response of fiber-reinforced incompressible non-linearly elastic solids, Int. J. Non-Linear Mech. 40 (2) (2005) 213–227.
[28] J. Merodio, G. Saccomandi, I. Sgura, The rectilinear shear of fiber-reinforced incompressible non-linearly elastic solids, Int. J. Non-Linear Mech. 42 (2) (2007) 342–354.
[29] R. Namani, P. Bayly, Shear wave propagation in anisotropic soft tissues and gels, IEEE Eng. Med. Biol. Soc. (2009) 1117–1122.
[30] R.W. Ogden, Incremental Statics and Dynamics of Pre-stressed Elastic Materials, 2007, pp. 1–26.
[31] P. Olver, Applications of Lie Groups to Differential Equations, vol. 107, Springer Verlag, New York, 2000.
[32] A. Ogden, W. Raymond, Non-linear elastic deformations, Dover, Mineola, New York, 1997.
[33] E. Pucci, G. Saccomandi, The anti-plane shear problem in nonlinear elasticity revisited, J. Elast. 113 (2) (2013) 167–177.
[34] R.S. Rivlin, Torsion of a rubber cylinder, J. Appl. Phys. 18 (1947) 444–449.
[35] J. Rodríguez, C. Ruiz, M. Doblaré, Mechanical stress in abdominal aortic aneurysms: influence of diameter, asymmetry, and material anisotropy, J. Biomech. Eng. 130 (2008) 021023.
[36] C. Rogers, G. Saccomandi, L. Vergori, Carroll-type deformations in nonlinear elastodynamics, J. Phys. A: Math. Theor. 47 (20) (2014) 205204.
[37] N. Rouze, M. Wang, M. Palmeri, K. Nightingale, Finite element modeling of impulsive excitation and shear wave propagation through in an incompressible transversely isotropic medium, J. Biomech. 46 (2013) 2761–2768.
[38] G. Saccomandi, Finite amplitude waves in nonlinear elastodynamics and related theories: a personal overview, in: Waves in Nonlinear Pre-Stressed Materials, Springer, Vien, New York, 2007, pp. 129–179.
[39] G. Saccomandi, R. Vitolo, On the mathematical and geometrical structure of the determining equations for shear waves in nonlinear isotropic incompressible elastodynamics, J. Math. Phys. 55 (8) (2014) 081502.
[40] L. Sandrin, B. Fourquet, J.M. Hasuqenoph, S. Yon, C. Fournier, F. Mal, C. Christidis, M. Zio, B. Poulet, F. Kazemi, M. Beaugrand, R. Palau, Transient elastography: a new noninvasive method for assessment of hepatic fibrosis, Ultrasound Med. Biol. 29 (2003) 1705–1713.
[41] A. Sarvazyan, O. Rudenko, S. Swanson, J. Fiowlkes, S. Emelianov, Shear wave elastic imaging: a new ultrasonic technique of medical diagnostics, Ultrasound Med. Biol. 24 (1998) 1419–1435.
[42] A.J.M. Spencer, Deformations of Fibre-Reinforced Materials, 1972.
[43] R. Thurston, Effective elastic coefficients for wave propagation in crystals under stress, J. Acoust. Soc. Am. 37 (2) (1965) 348–356.
[44] T. Tokuoka, M. Saito, Elastic wave propagations and acoustical birefringence in stressed crystals, J. Acoust. Soc. Am. 45 (5) (1969) 1241–1246.
[45] R. Toupin, B. Bernstein, Sound waves in deformed perfectly elastic materials. Acoustoelastic effect, J. Acoust. Soc. Am. 33 (2) (1961) 216–225.
[46] C. Truesdell, W. Noll, The Non-linear Field Theories of Mechanics, Springer, Berlin, Heidelberg, 2004.
[47] H. Tsai, P. Rosakis, On anisotropic compressible materials that can sustain elastodynamic anti-plane shear, J. Elast. 35 (1) (1994) 213–222.
[48] M. Valdez, B. Balachandran, Longitudinal nonlinear wave propagation through soft tissue, J. Mech. Behav. Biomed. Mater. 20 (2013) 192–208.